Design of Multi-Band Digital Filters and Full-Band Digital Differentiators Without Frequency Sampling and Iterative Optimization

Masayoshi Nakamoto, *Member, IEEE*, and Shuichi Ohno, *Senior Member, IEEE*

***Abstract*—Most design problems of digital filters (or differentiators) are formulated with a set of grid point in the frequency region (frequency sampling). These problems are usually difficult to solve, and often require iterative optimization. The objective of this paper is to provide an efficient and simplified design approach to multi-band filters (including low-pass filters or high-pass filters) as well as full-band differentiators. The proposed method does not require frequency sampling and iterative optimization to compute the coefficients of the filters or that of the differentiators. The magnitude and phase specifications are simultaneously approximated, and the errors in the specified frequency bands are controlled by using frequency-weighting factors. In addition, a maximum pole radius, which corresponds to a stability margin, can be specified to robustly ensure the stability of the filters or the differentiators. To evaluate the efficiency of proposed method, we compare the proposed method with several established methods. Simulation results show that, although the propose method does not utilize frequency sampling and iterative optimization, the designed filters and differentiators have sufficient performance.**

***Index Terms*—Full-band digital differentiators, infinite impulse response (IIR) filters, maximum pole radius, multi-band digital filters, no frequency sampling, no iterative optimization.**

I. Introduction

DIGITAL filters are essential elements of signal processing and have many applications in industrial electronics such as automatic control, communications engineering, and power system. A lot of papers on digital filters have been published in various journals [1]–[17], and the descriptions of digital filters are usually introduced in reference books [18]–[20]. According to the difference of structures, digital filters can be classified into two types; finite impulse response (FIR) filters [6], [14]–[17] and infinite impulse response (IIR) filters[2]–[5], [7]–[13]. Although FIR filters can achieve the exact linear phase property by the symmetrical coefficients and the guaranteed stability, the order of FIR filters is generally higher than that of IIR filters to reach the comparable accuracy. On the other hand, since the transfer function of IIR filters has the denominator polynomial, the location of the poles (stability condition) must be considered in the case of IIR filter design. In addition, to accomplish a simultaneous approximation for magnitude and phase responses, the problem needs a complex approximation which is generally more complicated than that of FIR filter design.

The impulse invariance method and the bilinear z transform method are well known as typical design methodologies for IIR filters [18]–[20]. Since the methods above are accomplished by transforming analog prototype filters (e.g., Butterworth filter and Chebyshev filter) to its equivalent digital filters, they are referred to as *indirect* methods. For convenience, we categorize the existing methods as in [2]–[5], [7]–[13] into *direct* methods for differentiating them from the indirect methods. One of the advantages of direct methods is to specify the arbitrary magnitude responses and phase characteristics (group delay). Hence, various types of filters with approximately linear phase can be derived by using direct methods. A prescribed maximum pole radius can also be given in order to achieve robust stability [7]. Consequently, direct methods demonstrate several functional advantages over indirect methods. However, the cost function usually requires a discrete set of frequency points: $\Omega_d = \{\omega'_1, \omega'_2, \ldots, \omega'_M\}$ where M indicates the number of the sampled points on the frequency region. (In this paper, this will be referred to as *frequency sampling*). One has to decide the appropriate M by taking into account the tradeoff between the computation cost and the performance.

The problems of IIR filter design by direct methods are often nonlinear optimization problems due to the presence of denominator polynomial in the approximation error. To solve the problem with stability constraints, the well-structured optimization schemes (e.g., quadratic programming [4], [7], and second-order cone programming [12]) have often been applied. Generally, direct methods require frequency sampling and/or iterative optimization. Due to the difficulty of the IIR filter design, several heuristic approaches to filter design have been proposed in [5], [9]–[11]. Although heuristic approaches have been successfully employed in filter designs, similar to some direct methods, heuristic approaches demand frequency sampling and iterative optimization. Also, some initial parameters such as population size, crossover rate, and mutation rate should often be selected by trial-and-error in order to have a good solution. Furthermore, the search performance of heuristic approaches generally depends on the size of problem. When the order of the filter is higher, the size of problem is increased. Then, it

Manuscript received May 16, 2013; revised August 28, 2013; accepted October 5, 2013. Date of publication November 13, 2013; date of current version March 21, 2014. This work was supported in part by a Research Grant from the Mazda Foundation, in part by the A-STEP program of the Japan Science and Technology Agency (JST), and in part by a Grant-in-Aid for Scientific Research (C) (25420372) from the Japan Society for the Promotion of Science (JSPS).

The authors are with the Department of System Cybernetics, Hiroshima University, Higashi-Hiroshima 739-8527, Japan (e-mail: masayoshi@ieee.org; ohno@hiroshima-u.ac.jp).

Color versions of one or more of the figures in this paper are available online at http://ieeexplore.ieee.org.

Digital Object Identifier 10.1109/TIE.2013.2290765

may be difficult to get a good result by heuristic approaches. Although direct methods and heuristic approaches are mainly studied in the field of digital filter design, indirect methods are still introduced as the representative of IIR filter design even in the recent technical books [18]–[20]. The reason may be that indirect methods do not require any complicated programming and the selection of initial parameters.

Digital differentiators are also an important class of digital filters, and several related works and applications have been published (see [3], [12], [21], [22] and the references therein). In this paper, we treat not only multi-band digital filters which include low-pass filters or high-pass filters but also full-band digital differentiators because they are well used in various situations. We show that the cost function can be expressed in a quadratic form with respect to the coefficients of the transfer function. It should be noted that the matrices associated with the quadratic forms are straightforward derived and the elements of the matrices can be integrable; hence, frequency sampling is not necessary in order to compute the matrices. Moreover, we introduce a novel optimization method without frequency sampling and iterative optimization, which is based on the newly proposed scheme: *relaxation of pole constraints* and *partial optimization*. Since our method does not require iterative optimization, then the selection of the initial point as well as the definition of the step size and the judgment of convergence is not necessary. Nevertheless, designers can specify the maximum pole radius and regulate the approximation error by frequency-weighting factors. Basically, the proposed scheme is for the IIR filter designs. However, if the order of denominator polynomial is 0, an FIR filter can be obtained.

The rest of this paper is organized as follows. We formulate the design problem of multi-band filters and full-band differentiators without frequency sampling in Section II. The proposed design scheme which does not require frequency sampling and iterative optimization is presented in Section III. To validate the proposed method, several design examples to compare our method with the existing methods are shown in Section IV. Finally, we give a conclusion in Section V.

II. Formulation of Design Problem Without Frequency Sampling

Let an input signal of the digital filter (differentiator) be $u(q)$ and its output signal be $y(q)$. Assume that $u(q)$ and $y(q)$ are both discrete signals which are sampled with the sampling period of T_s [s] in the time domain. Then, we have a difference equation

$$y(q) = -\sum_{k=1}^{m} a_k y(q-k) + \sum_{l=0}^{n} b_l u(q-l) \tag{1}$$

where a_k and b_l are the filter coefficients, and m and n are the orders of the filter (differentiator). Using the z-transformation of (1), we have a transfer function

$$H(z) = \frac{B(z)}{A(z)} = \frac{\sum_{l=0}^{n} b_l z^{-l}}{\sum_{k=0}^{m} a_k z^{-k}} \tag{2}$$

with $a_0 = 1$. Since the sampling period is T_s [s], we consider the range of frequency $0 \le f < 1/(2T_s)$ [Hz].

Here, $\omega = 2\pi f T_s$ and $\omega \in [0, \pi)$. Let the desired frequency response be $H_d(\omega)$ which is specified in $0 \le \omega < \pi$. Now, let $z = e^{j\omega}$ in (2) where $j^2 = -1$. Then, we consider the problem that approximates $H_d(\omega)$ with the rational transfer function $H(\omega)$. Here, the denominator polynomial $A(\omega)$ of order m and the numerator polynomial $B(\omega)$ of order n are, respectively expressed as

$$A(\omega) = \sum_{k=0}^{m} a_k e^{-jk\omega} \tag{3}$$

$$B(\omega) = \sum_{l=0}^{n} b_l e^{-jl\omega}. \tag{4}$$

Also, we define

$$\boldsymbol{a} := [a_0, a_1, \ldots, a_m]^T,\ a_0 = 1 \tag{5}$$

$$\boldsymbol{b} := [b_0, b_1, \ldots, b_n]^T \tag{6}$$

where the superscript T indicates the transposition of the matrix (vector).

Let the complex error function be $E(\omega) = H_d(\omega) - H(\omega)$. The problem of filter design is formulated to minimize the cost function of $E(\omega)$. Now, let the weighting function be $W(\omega)$ with $W(\omega) \ge 0$. For example, the weighted L_2 cost function is defined by $\int_0^\pi W(\omega)|E(\omega)|^2 d\omega$. Actually, with a discrete set of frequency points $\Omega_d = \{\omega'_1, \omega'_2, \ldots, \omega'_M\}$, then, the weighted L_2 cost function has to be approximated as $\sum_{\omega\in\Omega_d} W(\omega)|E(\omega)|^2$. This implies that frequency sampling is needed to solve the problem. In practice, the integral of the weighted L_2 cost function can be numerically computed by using discrete approximation (numerical integration). Since the main purpose of this work is to develop an easy-to-use alternative, we do not utilize frequency sampling.

Now, let us consider the cost function

$$J(\boldsymbol{a}, \boldsymbol{b}) = \int_0^\pi W(\omega)\left|H_d(\omega)A(\omega) - B(\omega)\right|^2 d\omega. \tag{7}$$

Similar to the other cost functions, the cost function (7) gets to 0 when $H_d(\omega)$ is well approximated by $A(\omega)$ and $B(\omega)$. Mullis and Roberts [2] introduced a method that approximates a given impulse response with $A(\omega)$ and $B(\omega)$ by minimizing (7), where $W(\omega) = 1$ for $\forall\omega \in [0, \pi)$. Since the ideal response is given by the impulse response, this is a filter design scheme in the *time* domain. In this paper, we treat an approximation problem of digital filter (differentiator) not in the time domain but in the *frequency* domain by using the cost function (7). We prove an integrability result in (7) for the design of multi-band digital filters and full-band digital differentiators. Accordingly, we derive the quadratic form of the cost function *without frequency sampling*.

A. Multi-Band Digital Filters

First, let us consider the multi-band (N-band) filters. We define the desired response such that

$$H_d(\omega) = F(\omega) := \begin{cases} G_1 e^{-j\tau_1\omega}, & \omega_1 \le \omega < \omega_2 \\ G_2 e^{-j\tau_2\omega}, & \omega_2 \le \omega < \omega_3 \\ \quad\vdots & \\ G_N e^{-j\tau_N\omega}, & \omega_N \le \omega < \omega_{N+1} \end{cases} \tag{8}$$

where $\omega_1, \omega_2, \ldots, \omega_{N+1}$ correspond to the band edge frequencies, $G_1, G_2, \ldots, G_N$ are the filter gains, and $\tau_1, \tau_2, \ldots, \tau_N$ are the desired group delays in the each band. We assume G_i and τ_i to be non-negative real values. It is natural that $F(\omega)$ includes the desired response of low-pass filters or high-pass filters.

Now, we assume the weighting function is

$$W(\omega) := \begin{cases} W_1, & \omega_1 \le \omega < \omega_2 \\ W_2, & \omega_2 \le \omega < \omega_3 \\ \quad\vdots & \\ W_N, & \omega_N \le \omega < \omega_{N+1} \end{cases} \tag{9}$$

where $W_1, W_2, \ldots, W_N$ are frequency-weighting factors and non-negative real values. As W_i gets larger, improved accuracy in $\omega_i \le \omega < \omega_{i+1}$ is achieved. Since $0 \le \omega < \pi$, we set $\omega_1 = 0$ and $\omega_{N+1} = \pi$. Note that $G_i =$ N/A and $\tau_i =$ N/A if $W_i = 0$, and $\tau_i =$ N/A if $G_i = 0$. Here, N/A stands for "not applicable."

Substituting (3), (4), (8), and (9) into (7), we obtain

$$J(\boldsymbol{a}, \boldsymbol{b}) = \sum_{i=1}^{N} W_i \int_{\omega_i}^{\omega_{i+1}} \Phi_i(\omega) d\omega \tag{10}$$

where

$$\Phi_i(\omega) = \left| G_i e^{-j\tau_i\omega} \sum_{k=0}^{m} a_k e^{-jk\omega} - \sum_{l=0}^{n} b_l e^{-jl\omega} \right|^2. \tag{11}$$

Using Euler's formula, (11) can be modified to

$$\begin{aligned} \Phi_i(\omega) = {} & G_i^2 \sum_{k=0}^{m}\sum_{k'=0}^{m} a_k a_{k'} \cos\left[(k-k')\omega\right] \\ & - 2G_i \sum_{k=0}^{m}\sum_{l=0}^{n} a_k b_l \cos\left[(k-l+\tau_i)\omega\right] \\ & + \sum_{l=0}^{n}\sum_{l'=0}^{n} b_l b_{l'} \cos\left[(l-l')\omega\right]. \end{aligned} \tag{12}$$

Then, substituting (12) into (10), we have

$$\begin{aligned} J(\boldsymbol{a}, \boldsymbol{b}) = {} & \sum_{k=0}^{m}\sum_{k'=0}^{m} a_k a_{k'} P_{k,k'} + 2\sum_{k=0}^{m}\sum_{l=0}^{n} a_k b_l Q_{k,l} \\ & + \sum_{l=0}^{n}\sum_{l'=0}^{n} b_l b_{l'} R_{l,l'} \end{aligned} \tag{13}$$

where

$$P_{k,k'} = \sum_{i=1}^{N} W_i G_i^2 \int_{\omega_i}^{\omega_{i+1}} \cos\left[(k-k')\omega\right] d\omega \tag{14}$$

$$Q_{k,l} = -\sum_{i=1}^{N} W_i G_i \int_{\omega_i}^{\omega_{i+1}} \cos\left[(k-l+\tau_i)\omega\right] d\omega \tag{15}$$

$$R_{l,l'} = \sum_{i=1}^{N} W_i \int_{\omega_i}^{\omega_{i+1}} \cos\left[(l-l')\omega\right] d\omega. \tag{16}$$

Let $P_{k,k'}$, $Q_{k,l}$ and $R_{l,l'}$ be the (k,k') element of $\boldsymbol{P}$ ($k, k' = 0, 1, \ldots, m$), the (k,l) element of $\boldsymbol{Q}$ ($k = 0, 1, \ldots, m$; $l = 0, 1, \ldots, n$) and the (l,l') element of $\boldsymbol{R}$ ($l, l' = 0, 1, \ldots, n$), respectively, where $\boldsymbol{P}$ is an $(m+1) \times (m+1)$ matrix, $\boldsymbol{Q}$ is an $(m+1) \times (n+1)$ matrix, and $\boldsymbol{R}$ is an $(n+1) \times (n+1)$ matrix. Then, (13) can be expressed in a quadratic form

$$J(\boldsymbol{a}, \boldsymbol{b}) = \boldsymbol{a}^T \boldsymbol{P} \boldsymbol{a} + 2\boldsymbol{a}^T \boldsymbol{Q} \boldsymbol{b} + \boldsymbol{b}^T \boldsymbol{R} \boldsymbol{b} \tag{17}$$

where $\boldsymbol{a}$ and $\boldsymbol{b}$ are, respectively, shown in (5) and (6). We get the quadratic form (17) with respect to the filter coefficients ($\boldsymbol{a}$ and $\boldsymbol{b}$). Here, it should be noted that $P_{k,k'}$, $Q_{k,l}$, and $R_{l,l'}$ are integrable, and the results are summarized in Table I without evaluating any integral. Hence, frequency sampling is not necessary to compute (14)–(16). Also, the elements of the matrices do not require any complex arithmetic; moreover, the group delays τ_i are embedded into $Q_{k,l}$. The contribution of the no frequency sampling is not only to achieve the simplicity but also to improve the design accuracy since any discrete approximation (or numerical integration) is not required.

B. Full-Band Digital Differentiators

Next, we consider the full-band differentiators. Since the response of the differentiators is different from that of the multi-band filters, we derive the matrices associated with the quadratic form again. The ideal response is given by

$$H_d(\omega) = D(\omega) := \frac{\omega}{\pi} e^{j(0.5\pi - \tau_d\omega)}, \quad \omega_1 \le \omega < \omega_{N+1} \tag{18}$$

with $\tau_d = \tau_s + 0.5$, where τ_s is an integer [3]. We assume $\omega_1 = 0$ and $\omega_{N+1} = \pi$. The weighting function is the same with (9).

Substituting (9) and (18) into (7), we can write

$$J(\boldsymbol{a}, \boldsymbol{b}) = \sum_{i=1}^{N} W_i \int_{\omega_i}^{\omega_{i+1}} \Psi(\omega) d\omega \tag{19}$$

where

$$\Psi(\omega) = \left| \frac{\omega}{\pi} e^{j(0.5\pi - \tau_d\omega)} \sum_{k=0}^{m} a_k e^{-jk\omega} - \sum_{l=0}^{n} b_l e^{-jl\omega} \right|^2. \tag{20}$$

TABLE I
ELEMENTS OF MATRICES IN THE MULTI-BAND FILTERS

$P_{k,k'}$	$\begin{cases} \sum_{i=1}^{N} W_i G_i^2 \cdot (\omega_{i+1} - \omega_i), & \text{if } k = k' \\ \sum_{i=1}^{N} W_i G_i^2 \frac{\sin[(k-k')\omega_{i+1}] - \sin[(k-k')\omega_i]}{k-k'}, & \text{otherwise} \end{cases}$
$Q_{k,l}$	$-\sum_{i=1}^{N} W_i G_i \widetilde{Q}_i$ where $\widetilde{Q}_i = \begin{cases} \omega_{i+1} - \omega_i, & \text{if } k = l - \tau_i \\ \frac{\sin[(k-l+\tau_i)\omega_{i+1}] - \sin[(k-l+\tau_i)\omega_i]}{k-l+\tau_i}, & \text{otherwise} \end{cases}$
$R_{l,l'}$	$\begin{cases} \sum_{i=1}^{N} W_i \cdot (\omega_{i+1} - \omega_i), & \text{if } l = l' \\ \sum_{i=1}^{N} W_i \frac{\sin[(l-l')\omega_{i+1}] - \sin[(l-l')\omega_i]}{l-l'}, & \text{otherwise} \end{cases}$

Using Euler's formula again, (20) can be modified to

$$\Psi(\omega) = \frac{\omega^2}{\pi^2} \sum_{k=0}^{m} \sum_{k'=0}^{m} a_k a_{k'} \cos\left[(k-k')\omega\right] - \frac{2\omega}{\pi} \sum_{k=0}^{m} \sum_{l=0}^{n} a_k b_l \sin\left[(k-l+\tau_d)\omega\right] + \sum_{l=0}^{n} \sum_{l'=0}^{n} b_l b_{l'} \cos\left[(l-l')\omega\right]. \quad (21)$$

Now, we let

$$P_{k,k'} = \frac{1}{\pi^2} \sum_{i=1}^{N} W_i \int_{\omega_i}^{\omega_{i+1}} \omega^2 \cos\left[(k-k')\omega\right] d\omega \quad (22)$$

$$Q_{k,l} = -\frac{1}{\pi} \sum_{i=1}^{N} W_i \int_{\omega_i}^{\omega_{i+1}} \omega \sin\left[(k-l+\tau_d)\omega\right] d\omega \quad (23)$$

$$R_{l,l'} = \sum_{i=1}^{N} W_i \int_{\omega_i}^{\omega_{i+1}} \cos\left[(l-l')\omega\right] d\omega. \quad (24)$$

Then, substituting (21) into (19), similar to the case of the multi-band filters, (19) can also be expressed in quadratic form (17), where the elements of matrices are (22)–(24). Using a partial integral, $P_{k,k'}$, $Q_{k,l}$, and $R_{l,l'}$ can be evaluated as in Table II (center column) without computing any integral; hence, frequency sampling is not needed. If $W(\omega) = 1$ for $\forall \omega \in [0, \pi)$, (22)–(24) are simply expressed as in Table II (right column). Hence, we recommend to refer to Table II (right column) if $W(\omega)$ is not employed.

III. DESIGN SCHEME WITHOUT FREQUENCY SAMPLING AND ITERATIVE OPTIMIZATION

In this section, we propose a design scheme without frequency sampling and iterative optimization. First, we define $K = m + n + 1$. Now, we rewrite (17) by redefining a $(K+1)$-dimensional vector as

$$\boldsymbol{x} := \begin{bmatrix} \boldsymbol{a} \\ \boldsymbol{b} \end{bmatrix} = \left[1, \underbrace{a_1, \ldots, a_m, b_0, b_1, \ldots, b_n}_{K \text{ components}} \right]^T \quad (25)$$

and a $(K+1) \times (K+1)$ square matrix as

$$\boldsymbol{S} := \begin{bmatrix} \boldsymbol{P} & \boldsymbol{Q} \\ \boldsymbol{Q}^T & \boldsymbol{R} \end{bmatrix} \quad (26)$$

where $m \geq 1$. Note that if $m = 0$, i.e., $A(\omega) = 1$, we obtain the FIR digital filter whose coefficients are computed by

$$\boldsymbol{b}_{\text{FIR}} = -\boldsymbol{R}^{-1} [Q_{00}, Q_{01}, \ldots, Q_{0,n}]^T. \quad (27)$$

From (25) and (26) with $m \geq 1$, (17) can be written as

$$J(\boldsymbol{x}) = \boldsymbol{x}^T \boldsymbol{S} \boldsymbol{x} \quad (28)$$

where $\boldsymbol{x} \in \Re^{K+1}$ and $\Re$ is a set of the real (continuous) valued coefficients. It is clear that $\boldsymbol{P} = \boldsymbol{P}^T$ and $\boldsymbol{R} = \boldsymbol{R}^T$. It follows that $\boldsymbol{S}$ is also a symmetric matrix, i.e., $\boldsymbol{S} = \boldsymbol{S}^T$. Also, it is obvious from (7) that $J(\boldsymbol{x}) \geq 0$ since $W(\omega) \geq 0$ and $|H_d(\omega)A(\omega) - B(\omega)|^2 \geq 0$. Hence, $\boldsymbol{S}$ is positive semidefinite. Now let us discuss the case when $J(\boldsymbol{x}) = 0$. It follows from (7) that the cases of $J(\boldsymbol{x}) = 0$ are equivalent to $H_d(\omega)A(\omega) - B(\omega) = 0$ i.e., $H(\omega) = H_d(\omega)$ or $W(\omega) = 0$ throughout $0 \leq \omega < \pi$. However, this case is hardly ever except for some special cases: $H_d(\omega)$ is constant or zero for $\forall \omega \in [0, \pi)$. Hence,

TABLE II
ELEMENTS OF MATRICES IN THE FULL-BAND DIFFERENTIATORS

	General case	Special case: $W(\omega)=1$ for $\forall\omega\in[0,\pi)$
$P_{k,k'}$	$\begin{cases} \frac{1}{3\pi^2}\sum_{i=1}^{N} W_i\cdot(\omega_{i+1}^3-\omega_i^3), & \text{if } k=k' \\ \frac{1}{\pi^2}\sum_{i=1}^{N} W_i\Big\{\frac{\omega_{i+1}^2\sin\left[(k-k')\omega_{i+1}\right]-\omega_i^2\sin\left[(k-k')\omega_i\right]}{k-k'} & \\ +2\frac{\omega_{i+1}\cos[(k-k')\omega_{i+1}]-\omega_i\cos[(k-k')\omega_i]}{(k-k')^2} & \\ -2\frac{\sin[(k-k')\omega_{i+1}]-\sin[(k-k')\omega_i]}{(k-k')^3}\Big\}, & \text{otherwise} \end{cases}$	$\begin{cases} \frac{\pi}{3}, & \text{if } k=k' \\ \frac{2\cos\left[(k-k')\pi\right]}{\pi(k-k')^2}, & \text{otherwise} \end{cases}$
$Q_{k,l}$	$\frac{1}{\pi}\sum_{i=1}^{N} W_i\Big\{\frac{\omega_{i+1}\cos\left[(k-l+\tau_d)\omega_{i+1}\right]-\omega_i\cos\left[(k-l+\tau_d)\omega_i\right]}{k-l+\tau_d}$ $-\frac{\sin[(k-l+\tau_d)\omega_{i+1}]-\sin[(k-l+\tau_d)\omega_i]}{(k-l+\tau_d)^2}\Big\}$	$\frac{\cos\left[(k-l+\tau_d)\pi\right]}{k-l+\tau_d}-\frac{\sin[(k-l+\tau_d)\pi]}{\pi(k-l+\tau_d)^2}$
$R_{l,l'}$	$\begin{cases} \sum_{i=1}^{N} W_i\cdot(\omega_{i+1}-\omega_i), & \text{if } l=l' \\ \sum_{i=1}^{N} W_i\frac{\sin[(l-l')\omega_{i+1}]-\sin[(l-l')\omega_i]}{l-l'}, & \text{otherwise} \end{cases}$	$\begin{cases} \pi, & \text{if } l=l' \\ 0, & \text{otherwise} \end{cases}$

we assume in fact that $J(\boldsymbol{x})\neq 0$, namely, $J(\boldsymbol{x})>0$. Thus, in this paper, we assume that $\boldsymbol{S}$ is positive definite.

Let us consider the problem which minimizes the quadratic function under the constraints that the all poles are inside or on a specified circle C with radius $r_{\rm c}$ where $0<r_{\rm c}<1$. The denominator polynomial $A(\omega)$ of order m has m poles denoted by $\rho_1,\rho_2,\ldots,\rho_m$. Then, the problem can be defined as follows:

$$\min_{\boldsymbol{x}} \quad \boldsymbol{x}^T\boldsymbol{S}\boldsymbol{x} \tag{29a}$$

$$\text{subject to} \quad \max\{|\rho_1|,|\rho_2|,\ldots,|\rho_m|\}\le r_{\rm c} \tag{29b}$$

where $\boldsymbol{x}\in\Re^{K+1}$. Equation (29b) indicates the stability constraints with prescribed stability margin.

To ensure the stability, for example, the positive realness of denominator, i.e., $\mathrm{Re}\{A(\omega)\}>0$, is applied [3], [4]. However, to achieve the positive realness, a discrete set of $A(\omega)$ for $\omega\in\Omega_d$ is necessary. This means that frequency sampling is also required when using the condition of positive realness. Also, in [7], Rouché's theorem with an iteration is employed to solve the problem. In this section, we propose a new approach to solve the problem (29) without using frequency sampling and iterative optimization.

A. Relaxation of Pole Constraints

Since problem (29) is hard to solve, we first *relax* (or neglect) the pole constraints (29b), which will be referred to as *relaxation of pole constraints*. After the *relaxation of pole constraints*, we force the pole constraints on the *relaxed* problem. Then, the problem with *relaxation of pole constraints* is expressed as

$$\min_{\boldsymbol{x}} \quad \boldsymbol{x}^T\boldsymbol{S}\boldsymbol{x} \tag{30a}$$

$$\text{subject to} \quad \left[1,\ \underbrace{0,0,\ldots,0}_{K\text{ components}}\right]\boldsymbol{x}=1 \tag{30b}$$

where $\boldsymbol{x}\in\Re^{K+1}$. The constraint (30b) indicates $a_0=1$.

We define the vector obtained by deleting the first element of $\boldsymbol{x}$ be $\boldsymbol{v}$, i.e.,

$$\boldsymbol{x}=\begin{bmatrix}1\\ \boldsymbol{v}\end{bmatrix} \tag{31}$$

where

$$\boldsymbol{v}:=\left[\underbrace{a_1,a_2,\ldots,a_m,b_0,b_1,\ldots,b_n}_{K\text{ components}}\right]^T. \tag{32}$$

That is, $\boldsymbol{v}$ is the K-dimensional vector and $\boldsymbol{v}\in\Re^K$. We define the first row except for the first element of $\boldsymbol{S}$ as $\overline{\boldsymbol{q}}$ and let the matrix obtained by deleting the first row and column of $\boldsymbol{S}$ be $\overline{\boldsymbol{R}}$. Then, $\overline{\boldsymbol{q}}$ is a $1\times K$ matrix, $\overline{\boldsymbol{R}}$ is a $K\times K$ matrix, and $\boldsymbol{S}$ can be written as

$$\boldsymbol{S}=\left[\begin{array}{c|c} P_{00} & \overline{\boldsymbol{q}} \\ \hline \overline{\boldsymbol{q}}^T & \overline{\boldsymbol{R}}\end{array}\right]. \tag{33}$$

Substituting (31) and (33) into (28), we can write

$$J(\boldsymbol{v})=P_{00}+2\overline{\boldsymbol{q}}\boldsymbol{v}+\boldsymbol{v}^T\overline{\boldsymbol{R}}\boldsymbol{v}. \tag{34}$$

Then, the problem (30) can be changed to an unconstrained problem

$$\min_{\boldsymbol{v}} \qquad 2\overline{\boldsymbol{q}}\boldsymbol{v} + \boldsymbol{v}^T\overline{\boldsymbol{R}}\boldsymbol{v} \tag{35}$$

where $\boldsymbol{v} \in \Re^K$. Differentiating (34) with respect to $\boldsymbol{v}$, we have

$$\frac{\partial J(\boldsymbol{v})}{\partial \boldsymbol{v}} = 2\overline{\boldsymbol{q}}^T + 2\overline{\boldsymbol{R}}\boldsymbol{v}. \tag{36}$$

By equating the result of (36) to $\mathbf{0}$, where $\mathbf{0}$ is a zero matrix of appropriate dimension, the solution $\boldsymbol{v}^*$ that minimizes (34) can be obtained as

$$\left.\frac{\partial J(\boldsymbol{v})}{\partial \boldsymbol{v}}\right|_{\boldsymbol{v}=\boldsymbol{v}^*} = \mathbf{0}. \tag{37}$$

It follows from (36) and (37) that

$$\boldsymbol{v}^* = -\overline{\boldsymbol{R}}^{-1}\overline{\boldsymbol{q}}^T. \tag{38}$$

Now, we denote

$$\begin{bmatrix}\boldsymbol{a}^* \\ \boldsymbol{b}^*\end{bmatrix} = \begin{bmatrix}1 \\ \boldsymbol{v}^*\end{bmatrix} \tag{39}$$

where $\boldsymbol{a}^*$ is an $(m+1)$ dimensional vector and $\boldsymbol{b}^*$ is an $(n+1)$ dimensional vector. Since the elements of $\boldsymbol{a}^*$ correspond to the denominator coefficients, we can compute the *temporary* poles from $\boldsymbol{a}^*$. (The elements of $\boldsymbol{b}^*$ are not used in this step). When the order of the denominator polynomial is m, we get m temporary poles denoted by $\rho_1^*, \rho_2^*, \ldots, \rho_m^*$. Also, let the radius and angle of ρ_k^* be $|\rho_k^*|$ and θ_k^*, respectively, i.e.,

$$\rho_k^* := |\rho_k^*|\, e^{j\theta_k^*},\ k = 1, 2, \ldots, m. \tag{40}$$

B. Replacement of Poles

Without loss of generality, we assume the poles $\rho_1^*, \rho_2^*, \cdots, \rho_m^*$ are simple. Then, with a partial fraction expansion on the proper rational part of (2), $H(z)$ can be written as

$$H(z) = \sum_{k=1}^{m} \widetilde{H}_k\left(\rho_k^* z^{-1}\right) + \sum_{k=0}^{n-m} \beta_k z^{-k} \tag{41}$$

where

$$\widetilde{H}_k(\alpha) = \frac{\gamma_k}{1-\alpha} \tag{42}$$

and the second term in (41) can be obtained if $n \geq m$ [19].

Here, suppose that a pole ρ_λ^* is outside C. Let the new pole be $\overline{\rho}_\lambda$ which is located on C. Then, let us consider how to choose $\overline{\rho}_\lambda$ which minimizes the influence caused by the movement from ρ_λ^* to $\overline{\rho}_\lambda$. We define an absolute difference between $\widetilde{H}_\lambda(\overline{\rho}_\lambda z^{-1})$ and $\widetilde{H}_\lambda(\rho_\lambda^* z^{-1})$ as

$$\Delta\widetilde{H}_\lambda(z) := \left|\widetilde{H}_\lambda(\overline{\rho}_\lambda z^{-1}) - \widetilde{H}_\lambda\left(\rho_\lambda^* z^{-1}\right)\right|. \tag{43}$$

It follows from (41)–(43) that $\Delta\widetilde{H}_\lambda(z)$ is an absolute error of $H(z)$ due to the movement from ρ_λ^* to $\overline{\rho}_\lambda$.

Now, $\widetilde{H}_k(\overline{\rho}_k z^{-1})$ can be linearized with a Taylor series around $\rho_k^* z^{-1}$ such that

$$\widetilde{H}_\lambda(\overline{\rho}_\lambda z^{-1}) \simeq \widetilde{H}_\lambda\left(\rho_\lambda^* z^{-1}\right) + \left(\overline{\rho}_\lambda z^{-1} - \rho_\lambda^* z^{-1}\right)\widetilde{H}_\lambda^{(1)}\left(\rho_\lambda^* z^{-1}\right) \tag{44}$$

where $\widetilde{H}_\lambda^{(1)}(\alpha)$ is the first derivative of $\widetilde{H}_\lambda(\alpha)$. According to (43) and (44), we have

$$\Delta\widetilde{H}_\lambda(z) \simeq \left|\widetilde{H}_\lambda^{(1)}\left(\rho_\lambda^* z^{-1}\right)\right| \Delta\rho_\lambda \tag{45}$$

where

$$\Delta\rho_\lambda = |\overline{\rho}_\lambda - \rho_\lambda^*| \tag{46}$$

which is the distance between $\overline{\rho}_\lambda$ and ρ_λ^*. It follows from (45) that $\Delta\widetilde{H}_\lambda(z)$ can be nearly minimized by selecting $\overline{\rho}_\lambda$ which minimizes (46). Hence, we choose $\overline{\rho}_\lambda$ so that $\overline{\rho}_\lambda$ is the nearest point on C from ρ_λ^* in the sense of Euclidean distance. Moreover, in order to minimize the total influence due to the movement of poles, we apply the above principle to the replacement of the other poles. That is, the new poles are obtained by setting

$$\overline{\rho}_k = \begin{cases} r_{\mathrm{c}} e^{j\theta_k^*}, & \text{if } |\rho_k^*| > r_{\mathrm{c}} \\ \rho_k^*, & \text{otherwise} \end{cases} \tag{47}$$

for $k = 1, 2, \ldots, m$. Hence, in (40), $|\rho_k^*|$ is changed to r_{c} without changing θ_k^* if ρ_k^* is placed outside C. It is obvious that the new poles satisfy

$$\max\left\{|\overline{\rho}_1|, |\overline{\rho}_2|, \ldots, |\overline{\rho}_m|\right\} \leq r_{\mathrm{c}}. \tag{48}$$

With the new poles $\overline{\rho}_1, \overline{\rho}_2, \ldots, \overline{\rho}_m$, we obtain

$$\begin{aligned}(1-\overline{\rho}_1 z^{-1})(1-\overline{\rho}_2 z^{-1})\cdots(1-\overline{\rho}_m z^{-1}) \\ = 1 + \overline{a}_1 z^{-1} + \overline{a}_2 z^{-2} + \cdots + \overline{a}_m z^{-m}\end{aligned} \tag{49}$$

where $1, \overline{a}_1, \overline{a}_2, \ldots, \overline{a}_m$ are new denominator coefficients. We put the vector of the new denominator coefficients as

$$\overline{\boldsymbol{a}} := [1, \overline{a}_1, \overline{a}_2, \ldots, \overline{a}_m]^T. \tag{50}$$

Therefore, all poles of the polynomial with the coefficients (50) can be placed inside or on the specified circle C as in (48). Thanks to the replacement rule (47), the new denominator coefficients (50) are also real. r_{c} should be selected based on the stability margin. The stability margin is enlarged as r_{c} is small. However, r_{c} is a constraint in the filter design. Hence, it should be noted that there is a tradeoff between the stability margin and the performance.

C. Partial Optimization

When using the replacement rule (47), the denominator coefficients are changed from $\boldsymbol{a}^*$ to $\overline{\boldsymbol{a}}$. This leads to a loss of the optimality of the solution in the sense of minimizing (7), i.e., $J(\overline{\boldsymbol{a}}, \boldsymbol{b}^*) \geq J(\boldsymbol{a}^*, \boldsymbol{b}^*)$, even if the influence caused by the

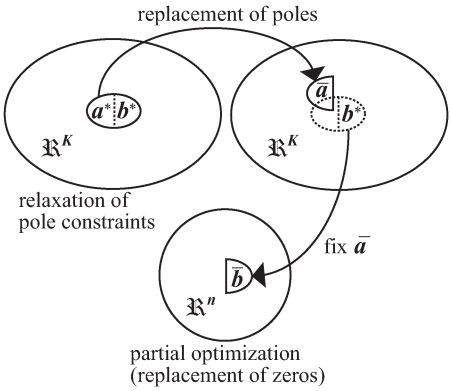

Fig. 1. Relaxation of pole constraints and partial optimization.

change of the poles is minimized. Hence, we can get a new $\boldsymbol{b}$ by solving a constraint problem

$$\min_{\boldsymbol{x}} \quad \boldsymbol{x}^T \boldsymbol{S} \boldsymbol{x} \tag{51a}$$

$$\text{subject to} \quad [\boldsymbol{I}_{m+1}\ \boldsymbol{0}]\boldsymbol{x} = \overline{\boldsymbol{a}} \tag{51b}$$

where $\boldsymbol{I}_{m+1}$ is an $(m+1)$-dimensional unit matrix, and $\boldsymbol{x} \in \Re^{m+n+2}$. In [13], an optimization scheme is presented based on the Lagrange multiplier method under the fixed denominator coefficients (50). In this paper, we show a different solution by a direct differentiation. Here, we regard (51) as a problem of *partial optimization*; i.e., we partially optimize the last $n+1$ components of $\boldsymbol{x}$, which corresponds to $\boldsymbol{b}$.

Now, we assume that $\overline{\boldsymbol{a}}$ is a constant vector independent of $\boldsymbol{b}$, and substitute $\overline{\boldsymbol{a}}$ into (17). It follows that the problem (51) can be changed to an unconstrained problem:

$$\min_{\boldsymbol{b}} \quad 2\overline{\boldsymbol{a}}^T \boldsymbol{Q} \boldsymbol{b} + \boldsymbol{b}^T \boldsymbol{R} \boldsymbol{b} \tag{52}$$

where $\boldsymbol{b} \in \Re^n$. Differentiating $J(\overline{\boldsymbol{a}}, \boldsymbol{b})$ with respect to $\boldsymbol{b}$, we have

$$\frac{\partial J(\overline{\boldsymbol{a}}, \boldsymbol{b})}{\partial \boldsymbol{b}} = 2\boldsymbol{R}\boldsymbol{b} + 2\boldsymbol{Q}^T \overline{\boldsymbol{a}}. \tag{53}$$

Let the solution of (52) be $\overline{\boldsymbol{b}}$, and equating the result of (53) to $\boldsymbol{0}$, i.e.,

$$\left.\frac{\partial J(\overline{\boldsymbol{a}}, \boldsymbol{b})}{\partial \boldsymbol{b}}\right|_{\boldsymbol{b}=\overline{\boldsymbol{b}}} = \boldsymbol{0}. \tag{54}$$

It follows from (53) and (54) that

$$\overline{\boldsymbol{b}} = -\boldsymbol{R}^{-1} \boldsymbol{Q}^T \overline{\boldsymbol{a}}. \tag{55}$$

Thus, the numerator coefficients (the elements of $\overline{\boldsymbol{b}}$) are obtained by the denominator coefficients (the elements of $\overline{\boldsymbol{a}}$) which correspond to the poles $\overline{\rho}_1, \overline{\rho}_2, \cdots, \overline{\rho}_m$. If $\overline{\boldsymbol{a}} = 1$ $(m = 0)$, (55) is equivalent to (27). Notice that $\overline{\boldsymbol{b}}$ is obtained as the optimal solution of (52). On the other hand, $\boldsymbol{b}^*$ is no longer the optimal solution of (52) due to the replacement of pole. This yields $J(\overline{\boldsymbol{a}}, \overline{\boldsymbol{b}}) \leq J(\overline{\boldsymbol{a}}, \boldsymbol{b}^*)$. Hence, (55) indicates the replacement of zeros when the denominator coefficients of $H(z)$ are fixed as (50). Fig. 1 illustrates the procedure of our method including the relationship of the relaxation of pole constraints and the partial optimization.

Our strategy is summarized as follows. First, (i) we neglect the pole constraints (29b) and compute the temporary poles $\rho_1^*, \rho_2^*, \cdots, \rho_m^*$ from $\boldsymbol{a}^*$ which is obtained from (38) and (39). Next, (ii) we replace the poles according to (47) with r_c, and get $\overline{\boldsymbol{a}}$ (the denominator coefficients) as in (49) and (50) so that the degradation of $H(z)$ can be minimized. Finally, (iii) we compute $\overline{\boldsymbol{b}}$ (the numerator coefficients) by (55), i.e., replace the zeros, in order to cancel the degradation of $H(z)$ which is caused by the movement of the poles. Then, it is preferable that the number of zeros is more than that of poles. According to [7], it is advantageous to choose $n \geq m$ since the poles ideally contribute only to the pass-bands, while zeros contribute to the pass-bands as well as to the stop-bands. Hence, our recommendation is to set $n \geq m$. Also, our optimization scheme does not require the decision of an initial point and a termination condition of the iteration. Since the proposed method initially obtains a stable IIR filter, the solution may be used as an initial solution to some other iterative methods.

IV. Design Examples

In this section, to evaluate the performance of our method, we present design examples of a two-band filter (*Example 1*) and a full-band differentiator (*Example 2*). We provide the comparisons between our method and the recently developed method [12] which needs frequency sampling and iterative optimization. We use the corresponding coefficients of the filter (or the differentiator) which are reported in [12]. Additionally, we present the comparisons with the indirect method in *Example 3* and *Example 4*. The design algorithm is implemented by MATLAB[1] program. For the factorization of polynomials (the computation of the poles $\rho_1^*, \rho_2^*, \cdots, \rho_m^*$ from $\boldsymbol{a}^*$) and the computation of (49), we use `roots` function and `poly` function of MATLAB, respectively.

A. Example 1

We design a two-band filter [8], [12] whose desired response is

$$H_d(\omega) = \begin{cases} e^{-j14.3\omega}, & 0 \leq \omega \leq 0.46\pi \\ 0.5e^{-j20\omega}, & 0.54\pi \leq \omega < \pi. \end{cases}$$

This is a good benchmark of multi-band filters since the gains and the group delays are, respectively, different in each band. We compare the proposed method with the existing method [12]. Similar to [12], we set $m = 6$, $n = 24$. The parameters are set to $N = 3$, $\omega_1 = 0$, $\omega_2 = 0.46\pi$, $\omega_3 = 0.54\pi$, $\omega_4 = \pi$, $W_1 = 1$, $W_2 = 0$, $W_3 = 1$, $G_1 = 1$, $G_3 = 0.5$, $\tau_1 = 14.3$, $\tau_3 = 20$, and $r_c = 0.945$. We compute the coefficients of the multi-band filter by using Table I. Comparison results of the magnitude responses and the group delays for the proposed and the existing method are depicted in Fig. 2. The values of (7) are computed as 8.8131e $-$ 06 (our method) and 6.0871e $-$ 04 (existing method), respectively. It can be observed from Fig. 2 that our method achieves a good performance despite no iterative optimization; however, the peak error is relatively large around the band-edge. The peak errors in the existing method

[1]MATLAB is a trademark of *The MathWorks Inc.*

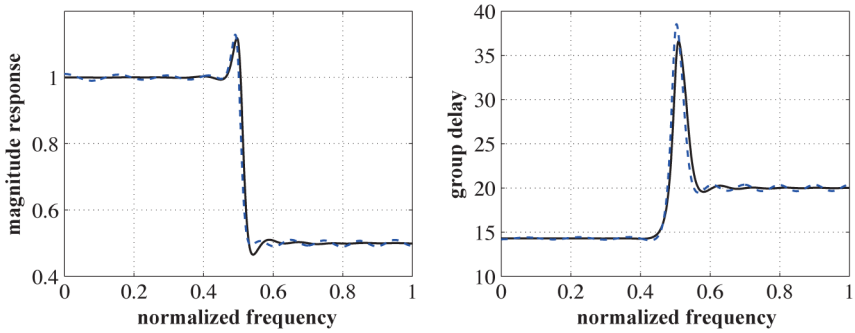

Fig. 2. Magnitude responses (left) and group delays (right) of our method (solid line) and the existing method (dashed line) in *Example 1*.

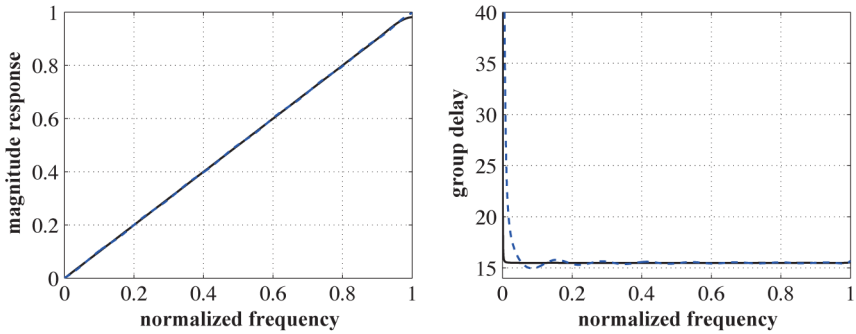

Fig. 3. Magnitude responses (left) and group delays (right) of our method (solid line) and the existing method (dashed line) in *Example 2*.

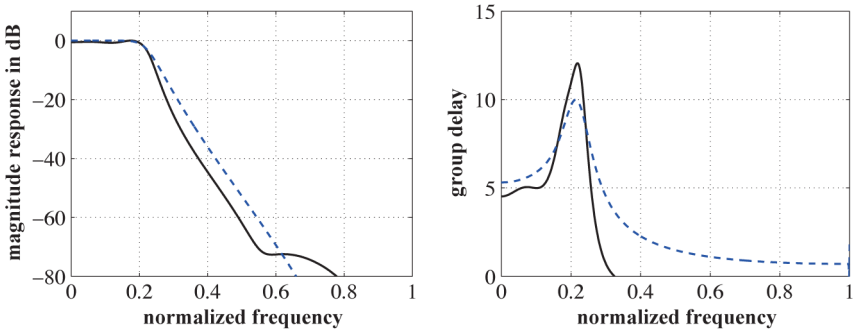

Fig. 4. Magnitude responses in dB (left) and group delays (right) of our method (solid line) and the Butterworth filter (dashed line) in *Example 3*.

are small in all the bands since the mini-max cost function is utilized. The peak errors in our method can be controlled by frequency-weighting factors. The obtained denominator coefficients of our filter are 1.0000e + 00, 7.8045e − 01, 1.5962e + 00, 9.6900e − 01, 6.7258e − 01, 2.5051e − 01, 5.0615e − 02. The corresponding numerator coefficients of our filter are −1.5049e − 03, 6.1225e − 04, 2.4457e − 03, −1.0805e − 03, −3.8799e − 03, 1.8924e − 03, 6.2132e − 03, −3.4534e − 03, −1.0451e − 02, 7.0278e − 03, 1.9757e − 02, −1.8302e − 02, −4.9617e − 02, 9.5702e − 02, 5.0574e − 01, 1.0158e + 00, 1.3137e + 00, 1.2174e + 00, 7.9762e − 01, 2.5466e − 01, 2.6172e − 01, −1.7748e − 01, 1.3184e − 01, −6.2149e − 02, 1.5710e − 02.

B. Example 2

We consider a full-band digital differentiator. The desired response is given by

$$H_d(\omega) = \frac{\omega}{\pi} e^{j(0.5\pi - \tau_d \omega)}, \qquad 0 \le \omega < \pi$$

TABLE III
MAXIMUM OF $|e_{\mathrm{R}}(\omega)|$ FOR $0 \le \omega \le 0.2\pi$ AND ATTENUATION FOR $\omega = 0.3\pi$ IN OUR FILTER AND THE BUTTERWORTH FILTER

	Our filter	Butterworth filter
maximum of $\lvert e_{\mathrm{R}}(\omega)\rvert$ for $0 \le \omega \le 0.2\pi$	0.0840	0.1087
attenuation (dB) for $\omega = 0.3\pi$	25.3048	17.6537

where $\tau_d = 14.5$ in [3], or $\tau_d = 15.5$ in [12]. Let us compare the proposed method with the existing method [12]. The orders of the digital differentiator are set to $m = n = 17$, which are the same as that of the existing method. We consider a case without weighting function ($W(\omega) = 1$ for $\forall \omega \in [0, \pi)$). The parameters are chosen as $\tau_s = 15$ and $r_c = 0.95$. The coefficients of the digital differentiator are computed by Table II (right column). We obtain the results as given in Fig. 3 including a comparison with the existing method. The values of (7) are computed as 5.1139e − 08 (our method) and 5.4123e − 05 (existing method), respectively. From Fig. 3 (left), it is hard to

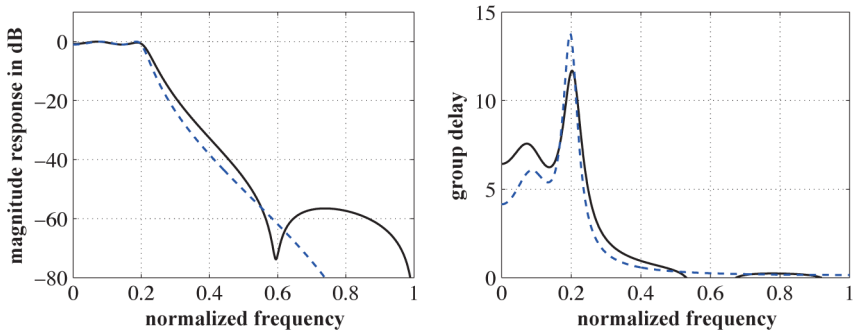

Fig. 5. Magnitude responses in dB (left) and group delays (right) of our method (solid line) and the Chebyshev filter (dashed line) in *Example 4*.

distinguish the difference between both methods; that is, the performance of two methods is almost similar. Also, it can be observed from Fig. 3 (right) that the group delay of the filter has a large error near the origin. However, as suggested in [12], the error can be neglected since the magnitude on the frequencies near the origin is almost 0. Hence, we suppose the proposed method achieves sufficient precision in terms of both the magnitude and phase for the design of full-band digital differentiators. The computed denominator coefficients of our differentiator are 1.0000e + 00, 1.0392e + 00, 6.4672e − 02, −1.0359e − 02, 3.4195e − 03, −1.6186e − 03, 7.8603e − 04, −5.4738e − 04, 2.6896e − 04, −2.6822e − 04, 1.0565e − 04, −1.6692e − 04, 3.9786e − 05, −1.2265e − 04, 9.1465e − 06, −1.0122e − 04, −5.8285e − 06, −9.1989e − 05. The corresponding numerator coefficients of our differentiator are −6.1187e − 05, 7.3065e − 05, −8.8414e − 05, 1.0864e − 04, −1.3589e − 04, 1.7359e − 04, −2.2738e − 04, 3.0707e − 04, −4.3073e − 04, 6.3412e − 04, −9.9499e − 04, 1.7047e − 03, −3.3232e − 03, 7.9875e − 03, −2.8789e − 02, 3.5965e − 01, 1.2783e − 02, −3.4940e − 01.

C. Example 3

We demonstrate the comparison with a Butterworth filter designed by bilinear z transform in the design of low-pass filter. The specifications of the low-pass filter are given as follows [19].

1) passband cutoff frequency: 0.2π
2) passband ripple: 1 dB ($\simeq$0.1087)
3) stopband cutoff frequency: 0.3π
4) stopband attenuation: 15 dB.

In order to satisfy the given specifications, the required orders of the Butterworth filter are $m = n = 6$. Hence, we also set the orders of our filter to $m = n = 6$. We compute the coefficients of the low-pass filter based on Table I where $N = 3$, $\omega_1 = 0$, $w_2 = 0.2\pi$, $w_3 = 0.3\pi$, $w_4 = \pi$, $W_1 = 20$, $W_2 = 0$, $W_3 = 1$, $G_1 = 1$, $G_3 = 0$, $\tau_1 = 5$ and $r_c = 0.90$. Now, the Butterworth filter (or the Chebyshev filter) satisfies a condition $|H(\omega)| \leq 1$. For fair comparison, we normalize the numerator coefficients of our filter to achieve $|H(\omega)| \leq 1$ by dividing the initially obtained numerator coefficients by its maximum value of $|H(\omega)|$. Fig. 4 indicates the comparison of magnitude responses in dB (left) and group delays (right) between our filter and the Butterworth filter. Now, let the passband magnitude ripple be $e_R(\omega) = 1 - |H(\omega)|$ for $0 \leq \omega \leq 0.2\pi$. Then, the maximum of $|e_R(\omega)|$ (an index of the accuracy in the passband) and the attenuation for $\omega = 0.3\pi$ (an index of the cutoff sharpness) in the both filters are given in Table III. From Table III, our filter attains the given specifications better than the Butterworth filter. However, our method is somewhat complex since the weighting factor W_1 should be selected. The obtained denominator coefficients of our filter are 1.0000e + 00, −4.2792e + 00, 8.2187e + 00, −8.9523e + 00, 5.8053e + 00, −2.1209e + 00, 3.4104e − 01. The corresponding (normalized) numerator coefficients of our filter are 3.5371e − 03, 3.1973e − 03, 2.2648e − 03, 1.1746e − 03, 4.3027e − 04, 3.5923e − 04, 9.4682e − 04.

TABLE IV
MAXIMUM OF $|e_R(\omega)|$ FOR $0 \leq \omega \leq 0.2\pi$ AND ATTENUATION FOR $\omega = 0.3\pi$ IN OUR FILTER AND THE CHEBYSHEV FILTER

	Our filter	Chebyshev filter
maximum of $\lvert e_R(\omega)\rvert$ for $0 \leq \omega \leq 0.2\pi$	0.1081	0.1087
attenuation (dB) for $\omega = 0.3\pi$	18.9008	23.6074

D. Example 4

In the final example, we show the comparison of our method with a Chebyshev filter (type I) where the specifications are the same as in *Example 3*. Then, the required orders of the Chebyshev filter are $m = n = 4$. Hence, we set the orders of our filter to $m = n = 4$ to be equal to the orders of the Chebyshev filter. Similar to *Example 3*, we normalize the numerator coefficients of our filter to satisfy $|H(\omega)| \leq 1$. With $N = 3$, $w_1 = 0$, $w_2 = 0.2\pi$, $w_3 = 0.3\pi$, $w_4 = \pi$, $W_1 = 150$, $W_2 = 0$, $W_3 = 1$, $G_1 = 1$, $G_3 = 0$, $\tau_1 = 7$, and $r_c = 0.92$, we compute the coefficients of the low-pass filter by using Table I. Fig. 5 shows the comparison of the magnitude responses in dB and the group delays between the both filters. Table IV shows the maximum error for $0 \leq \omega \leq 0.2\pi$ and the attenuation for $\omega = 0.3\pi$ in the both filters. We can see from Table IV that our filter satisfies the given specifications. Although the attenuation of our filter is worse than that of the Chebyshev filter, the phase linearity of our filter is better than that of the Chebyshev filter due to the simultaneous optimization of the magnitude and phase responses. The computed denominator coefficients of our filter are 1.0000e + 00, −2.9994e + 00, 3.6952e + 00, −2.1826e + 00, 5.1793e − 01. The corresponding (normalized) numerator coefficients of our filter are −6.8320e − 03, 1.8940e − 03, 9.0662e − 03, 1.2536e − 02, 1.1693e − 02.

V. Conclusion

We have formulated the design problems of multi-band digital filters and full-band digital differentiators. The design problems are expressed in the quadratic form with respect to the coefficients of the transfer function. The matrices associated with the quadratic forms are straightforward derived and it can be computed without any frequency sampling. Subsequently, we have proposed the novel design strategy with the relaxation of pole constraints and the partial optimization, which also does not require frequency sampling. Moreover, the scheme does not need iterative optimization. Since the prescribed stability margin can be given, the filters and differentiators designed by our method have robust stability. We have evaluated the performance of our method by comparing with the recently developed method, from which we can conclude that our method has comparable performance with the existing method. Hence, we have succeeded in providing the new easy-to-use option to design multi-band digital filters and full-band digital differentiators.

Acknowledgment

The authors would like to express sincere thanks to the anonymous reviewers for their valuable comments.

References

[1] D. R. Wilson, D. R. Corrall, and R. F. Mathias, "The design and application of digital filters," *IEEE Trans. Ind. Electron. Control Inst.*, vol. IECI-20, no. 2, pp. 68–74, May 1973.

[2] C. T. Mullis and R. A. Roberts, "The use of second-order information in the approximation of discrete-time linear systems," *IEEE Trans. Acoust., Speech, Signal Process.*, vol. ASSP-24, no. 3, pp. 226–238, Jun. 1976.

[3] A. T. Chottera and G. A. Jullien, "A linear programming approach to recursive digital filter design with linear phase," *IEEE Trans. Circuits Syst.*, vol. CAS-29, no. 3, pp. 139–149, Mar. 1982.

[4] W.-S. Lu, S.-C. Pei, and C.-C. Tseng, "A weighted least-squares method for the design of stable 1-D and 2-D IIR digital filters," *IEEE Trans. Signal Process.*, vol. 46, no. 1, pp. 1–10, Jan. 1998.

[5] K. S. Tang, K. F. Man, S. Kwong, and Z. F. Liu, "Design and optimization of IIR filter structure using hierarchical genetic algorithms," *IEEE Trans. Ind. Electron.*, vol. 45, no. 3, pp. 481–487, Jun. 1998.

[6] K.-K. Shyu and C.-Y. Chang, "Modified FIR filter with phase compensation technique to feedforward active noise controller design," *IEEE Trans. Ind. Electron.*, vol. 47, no. 2, pp. 444–453, Apr. 2000.

[7] M. C. Lang, "Least-squares design of IIR filters with prescribed magnitude and phase responses and a pole radius constraint," *IEEE Trans. Signal Process.*, vol. 48, no. 11, pp. 3109–3121, Nov. 2000.

[8] A. Tarczynski, G. D. Cain, E. Hermanowicz, and M. Rojewski, "A WISE method for designing IIR filters," *IEEE Trans. Signal Process.*, vol. 49, no. 7, pp. 1421–1432, Jul. 2001.

[9] J.-T. Tsai, J.-H. Chou, and T.-K. Liu, "Optimal design of digital IIR filters by using hybrid taguchi genetic algorithm," *IEEE Trans. Ind. Electron.*, vol. 53, no. 3, pp. 867–879, Jun. 2006.

[10] Y. Yu and Y. Xinjie, "Cooperative coevolutionary genetic algorithm for digital IIR filter design," *IEEE Trans. Ind. Electron.*, vol. 54, no. 3, pp. 1311–1318, Jun. 2007.

[11] C. Dai, W. Chen, and Y. Zhu, "Seeker optimization algorithm for digital IIR filter design," *IEEE Trans. Ind. Electron.*, vol. 57, no. 5, pp. 1710–1718, May 2010.

[12] A. Jiang and H. K. Kwan, "Minimax design of IIR digital filters using iterative SOCP," *IEEE Trans. Circuits Syst. I, Reg. Papers*, vol. 57, no. 6, pp. 1326–1337, Jun. 2010.

[13] M. Nakamoto and S. Ohno, "Closed-form approximation of linear phase IIR digital filters with guaranteed stability," in *Proc. IEEE ICASSP*, 2011, pp. 1645–1648.

[14] C. Rusu and B. Dumitrescu, "Iterative reweighted l1 design of sparse FIR filters," *Signal Process.*, vol. 92, no. 4, pp. 905–911, Apr. 2012.

[15] A. Jiang, H. K. Kwan, and Y. Zhu, "Peak-error-constrained sparse FIR filter design using iterative SOCP," *IEEE Trans. Signal Process.*, vol. 60, no. 8, pp. 4035–4044, Aug. 2012.

[16] F. A. S. Neves, H. E. P. de Souza, M. C. Cavalcanti, F. Bradaschia, and E. J. Bueno, "Digital filters for fast harmonic sequence component separation of unbalanced and distorted three-phase signals," *IEEE Trans. Ind. Electron.*, vol. 59, no. 10, pp. 3847–3859, Oct. 2012.

[17] A. Jiang and H. K. Kwan, "WLS design of sparse FIR digital filters," *IEEE Trans. Circuits Syst. I, Reg. Papers*, vol. 60, no. 1, pp. 125–135, Jan. 2013.

[18] A. V. Oppenheim and R. W. Schafer, *Discrete-Time Signal Processing*. Upper Saddle River, NJ, USA: Prentice-Hall, Aug. 2009.

[19] V. K. Ingle and J. G. Proakis, *Digital Signal Processing Using MATLAB*. Stamford, CT, USA: Cengage Learning, Jan. 2011.

[20] S. K. Mitra, *Digital Signal Processing*. New York, NY, USA: McGraw-Hill, Jun. 2011.

[21] W. Chen and M. Saif, "Output feedback controller design for a class of MIMO nonlinear systems using high-order sliding-mode differentiators with application to a laboratory 3-D crane," *IEEE Trans. Ind. Electron.*, vol. 55, no. 11, pp. 3985–3997, Nov. 2008.

[22] M. Iqbal, A. I. Bhatti, S. I. Ayubi, and Q. Khan, "Robust parameter estimation of nonlinear systems using sliding-mode differentiator observer," *IEEE Trans. Ind. Electron.*, vol. 58, no. 2, pp. 680–689, Feb. 2011.

Masayoshi Nakamoto (M'00) received the B.E. and M.E. degrees from Okayama University of Science, Okayama, Japan, in 1997 and 1999, respectively, and the Dr.Eng. degree from Hiroshima University, Higashi-Hiroshima, Japan, in 2002.

From April 2002 to March 2005, he was a JSPS Research Fellow. He is currently an Assistant Professor in the Department of System Cybernetics, Hiroshima University. His research interests are in the areas of digital signal processing and control engineering.

Shuichi Ohno (M'95–SM'11) received the B.E., M.E., and Dr.Eng. degrees in applied mathematics and physics from Kyoto University, Kyoto, Japan, in 1990, 1992, and 1995, respectively.

From 1995 to 1999, he was a Research Associate in the Department of Mathematics and Computer Science, Shimane University, Shimane, Japan. He is currently an Associate Professor in the Department of System Cybernetics, Hiroshima University, Higashi-Hiroshima, Japan. His current interests are in the areas of signal processing for communications and adaptive signal processing.